

# The removal of Cu(II) and Co(II) from aqueous solutions using cross-linked chitosan—Evaluation by the factorial design methodology

Antonio R. Cestari<sup>a,\*</sup>, Eunice F.S. Vieira<sup>a</sup>,  
Iataanderson A. de Oliveira<sup>a</sup>, Roy E. Bruns<sup>b</sup>

<sup>a</sup> *Laboratory of Materials and Calorimetry, Departamento de Química/CCET, Universidade Federal de Sergipe, CEP 49100-000 São Cristóvão, Sergipe, Brazil*

<sup>b</sup> *Universidade Estadual de Campinas, Instituto de Química, CP 6154, 13083-970 Campinas, São Paulo, Brazil*

Received 31 May 2006; received in revised form 27 July 2006; accepted 28 August 2006

Available online 1 September 2006

## Abstract

A 2<sup>3</sup> factorial design was employed to evaluate the quantitative removal of Cu(II) and Co(II) on glutaraldehyde-cross-linked chitosan from kinetic isotherms, using chitosan masses of 100 and 300 mg and temperatures of 25 and 35 °C. The adsorption parameters were analyzed statistically using modeling polynomial equations and a cumulative normal probability plot. The results indicated the higher quantitative preference of the chitosan for Cu(II) in relation to Co(II). Increasing the chitosan mass decreases the adsorption/mass ratio (mol g<sup>-1</sup>) for both metals. The principal effect of the temperature did not show statistical importance. The adsorption thermodynamic parameters, namely  $\Delta_{\text{ads}}H$ ,  $\Delta_{\text{ads}}G$  and  $\Delta_{\text{ads}}S$ , were determined. Exothermic and endothermic results were found in relation to a specific factorial design experiment. A comparison of  $\Delta_{\text{ads}}H$  values was made in relation to some metal–adsorbent interactions in literature. It is suggested that the adsorption thermodynamic parameters are determined by the influence of the principal and interactive experimental parameters and not by the temperature changes alone.

© 2006 Elsevier B.V. All rights reserved.

**Keywords:** Removal of metals; Chitosan; Adsorption thermodynamics; Chemometrics

## 1. Introduction

Metals from aqueous and non-aqueous solutions have become increasingly important in many industries, including battery and power storage, coatings, electroplating, and power industries. Traditional metal elimination are often of limited effectiveness in order to decrease allowable levels specified by regulatory agencies [1]. These metals inevitably make their way into plant discharge streams in at least dilute concentrations, despite application of remediation technologies [2]. The limitations and cost of traditional treatment methods has led researchers to search for alternative treatments. One promising area of development has been adsorption.

Activated carbon is the most common adsorbent due to its effectiveness, versatility, and good capacity for the adsorption

of metals, dyes and other organic compounds. However, it suffers from a number of disadvantages, mainly its high cost on large-scale uses [3]. This has led many workers to search for the use of cheap and efficient alternative adsorbent materials such as the biopolymers chitin and chitosan [4].

Chitin is a biodegradable and nontoxic polysaccharide widely spread among marine and terrestrial invertebrates and fungi [3,4]. It is usually obtained from waste materials of the sea food-processing industry, mainly shells of crab, shrimp, prawn and krill. Its isolation calls for chemical treatments to eliminate natural contaminants, such as inorganics, proteins, lipids and pigments. By treating crude chitin with aqueous 40–50% sodium hydroxide in the 383–388 K range chitosan is obtained. Chitin and chitosan are closely related since both are linear polysaccharides containing 2-acetamido-2-deoxy-D-glucopyranose and 2-amino-2-deoxy-D-glucopyranose units joined by  $\beta(1 \rightarrow 4)$  glycosidic bonds [5]. The chemical and physical properties of these polymers are different in nature

\* Corresponding author. Tel.: +55 79 32126656; fax: +55 79 32126684.  
E-mail address: [cestari@ufs.br](mailto:cestari@ufs.br) (A.R. Cestari).

and the fully deacetylated product is rarely obtained due to the risks of chain depolymerization [6].

Applications for chitosan currently are found in industrial wastewater treatment and in recovery of feedgrade material from food processing plants [7]. Numerous studies have demonstrated the effectiveness of chitosan and its derivative products in the uptake of metals, such as lead, cadmium, copper, nickel and oxyanions, as well as complexed metal ions. In other areas, chitosan has been employed as an excellent adsorbent for sorption of phenols and polychlorinated biphenyls [8], enzymes [9], protein separations [10], and in enzyme immobilizations procedures and Cu(II) removal [11,12].

The magnitude of metal adsorption depends on the source of chitosan, the degree of deacetylation, the nature of the adsorbate molecules, and solution conditions, such as the type of solvent, which makes experimental procedures the only manner to evaluate the interaction chitosan–adsorbate molecule. However, the principal and/or interactive roles of the experimental adsorption parameters, which have been considered important to analyze and to optimize further kinetics and thermodynamics adsorption modelings are still lacking in this specific chitosan adsorption field.

Since many interactions of the experimental adsorption variables are frequently evidenced, which can predominate over main factor effects, univariate optimization strategies have been shown to be relatively inadequate in these kinds of adsorption studies. Statistical methods of experimental design and system optimization such as factorial design and response surface analysis have been applied to different adsorption systems because of their capacities to extract relevant information from systems while requiring a minimum number of experiments. Examples of recent applications of the factorial design methodology in adsorption at solid/solution interfaces are found, for example, in the interaction of non-ionic dispersant on lignite particles [13], removal of Ga(III) from aqueous solution using bentonite [14], adsorption of cationic dye on activated carbon beads [15], and optimization of solid-phase extraction and separation of metabolites using HPLC [16]. Multivariate methods are capable of measuring interaction effects on metal adsorption as well as the individual effect of each experimental factor on response properties of interest in the most precise way possible. However, to our knowledge, despite the large number of works concerning adsorption of metals on chitosan, the importance of experimental parameters, such as the amount of chitosan and temperature, as well as their interactions, has been relatively little studied and compared from the thermodynamic viewpoint.

In this work, chitosan was cross-linked with glutaraldehyde to improve its chemical and mechanical features. A factorial design was used to evaluate the importance of some experimental factors concerning the adsorption quantities and the thermodynamical adsorption parameters of Cu(II) and Co(II) on cross-linked chitosan from aqueous solutions. The factorial design required the execution of a relatively small number of distinct experiments. To determine the statistical significance of the evaluated effects, duplicate determinations were made for each of these experiments.

## 2. Materials and methods

### 2.1. Materials and preliminary characterization of the raw chitosan sample

Water was used after bidistillation. The copper and cobalt chloride salts (Aldrich) were dried in a vacuum line at 413 K for 8 h. Glutaraldehyde (Sigma), 25% aqueous solution, was used without purification.

The chitosan powder used was from fresh Norwegian shrimp shells from Primex Ingredients A.S. (free of charge, Norway). The following characterizations were performed (details not shown), in order to check some important aspects, concerning the purity and structural aspects of the chitosan sample: the degree of deacetylation (%) was determined by infrared spectroscopy [17,18]. Solid-state  $^{13}\text{C}$  NMR spectroscopy was used to verify the purity of the chitosan sample by the positions and their respective intensities of the  $^{13}\text{C}$  absorption peaks, from 20 to 200 ppm [18]. The total quantity of nitrogen (% and  $\text{mol g}^{-1}$ ) was determined by the Kjeldhal method.

The raw chitosan powder was cross-linked using a 2% (m/v) glutaraldehyde solution as described earlier [18]. Fig. 1 shows a schematic view of the glutaraldehyde-modified chitosan cross-linking reaction. The cross-linked chitosan was sieved and used in the 60–100 mesh range and conditioned in a dark air-free flask, in order to prevent possible interactions between the amine groups and atmospheric  $\text{CO}_2$  [19].

The thermogravimetric analyses (TG and DTG) were made using about 10 mg of material, under nitrogen atmosphere from 25 to 600 °C, in a SDT 2960 thermoanalyzer, from TA Instruments. The X-ray analyses were performed in a Rigaku diffractometer, in the  $2\theta$  range from 5° to 80° (accumulation rate of 0.02°  $\text{min}^{-1}$ ).

### 2.2. Adsorption experiments

The adsorptions of the metals were performed using batch procedures [20], where the chitosan quantities specified by the adsorption factorial design were placed in contact with 50 mL of aqueous solutions at  $5.0 \times 10^{-3} \text{ mol L}^{-1}$  in 100 mL polyethylene flasks at 25 or 35 °C, according to the adsorption factorial design matrix in Table 1. The suspensions were agitated for 120 min, sufficient time to reach equilibrium, according to the kinetic isotherms results (Fig. 2), which were performed using the same experimental conditions of each factorial design experiment.

Table 1  
Factors and levels used in the  $2^3$  factorial design study

Factors	Levels	
	(–)	(+)
Quantity of chitosan, $Q$ (mg)	100	300
Type of metal, $M$ ( $\text{MCl}_2$ salts)	$\text{Cu}^{2+}$	$\text{Co}^{2+}$
Temperature, $T$ (°C)	25	35

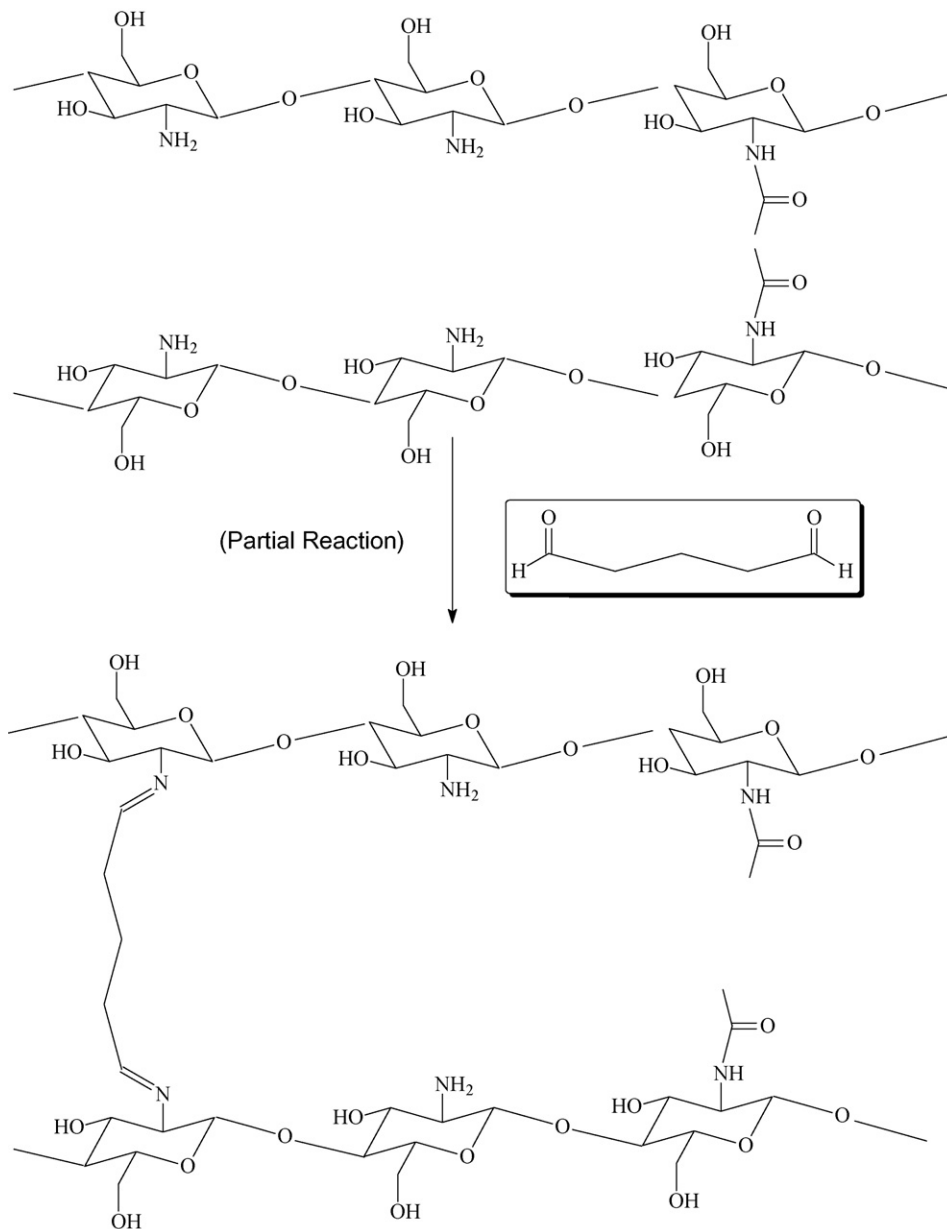


Fig. 1. Partial cross-linking reaction of chitosan using glutaraldehyde.

Supernatant aliquots were collected using a vacuum filtration system and analyzed by back-titration in duplicate or triplicate runs using standard  $0.01 \text{ mol L}^{-1}$  EDTA and  $\text{Zn}^{2+}$  solutions [21,22].

The adsorbed metals quantities were calculated using the expression [22,23]:

$$N_f = \frac{(C_i - C_e)V}{m} \quad (1)$$

where  $N_f$  is the fixed quantity of metal per gram of chitosan at equilibrium in mol/g,  $C_i$  the initial concentration of metal in mol/L,  $C_e$  the concentration of metal present at equilibrium in mol/L,  $V$  the volume of the solution in L, and  $m$  is the mass of chitosan in grams.

The statistical calculations (one- and two-population  $t$ -tests,  $F$ -test, analysis of variance (ANOVA) and multiple regressions) were performed using the ORIGIN<sup>®</sup>, release 6.0 software and the Statistica<sup>®</sup> software package [23,24].

### 3. Results and discussion

#### 3.1. Initial considerations

The amount of nitrogen of the chitosan, before and after the cross-linking reaction, showed the presence of  $6.77 \pm 0.30\%$  ( $4.84 \pm 0.25 \text{ mmol g}^{-1}$ ) and  $6.50 \pm 0.34\%$  ( $4.42 \pm 0.25 \text{ mmol g}^{-1}$ ) of nitrogen. The TG and DTG curves of both the non-cross linked and cross-linked chitosan are shown in Fig. 3 and the XRD diffractograms of the non-cross

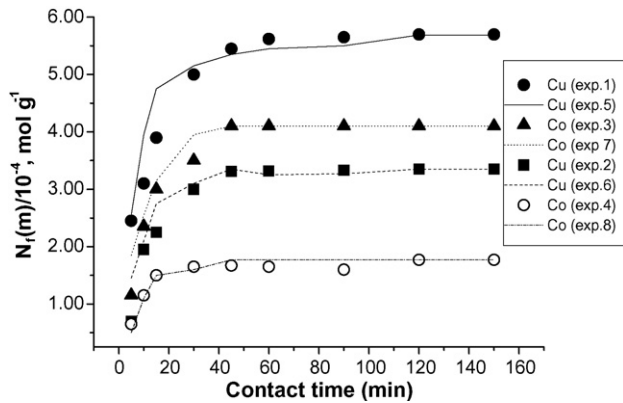


Fig. 2. Kinetic isotherms of the adsorption of the metals into the cross-linked chitosan at the same conditions of the factorial design matrix. Experiments 1, 2, 5 and 6 are related to Cu(II) and experiments 3, 4, 7 and 8 are related to Co(II).

linked and cross-linked chitosan are shown in Fig. 4. From the thermal analysis and XRD results, the chemical structures of both non-cross linked and cross-linked materials seem to be rather similar each other.

Adsorption using chitosan occurs not only on the nitrogenated and oxygenated groups of the chitosan external surface, but also at sites throughout the bulk of the chitosan as a consequence of solution infiltration into the internal parts of the material [3,4].

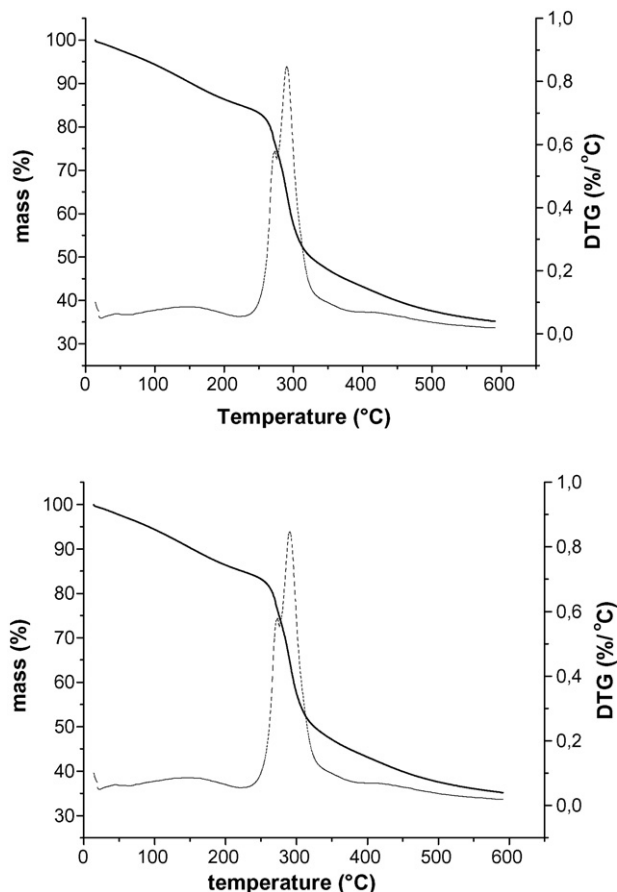


Fig. 3. TG/DTG curves of the raw chitosan (upper panel) and cross-linked chitosan (lower panel).

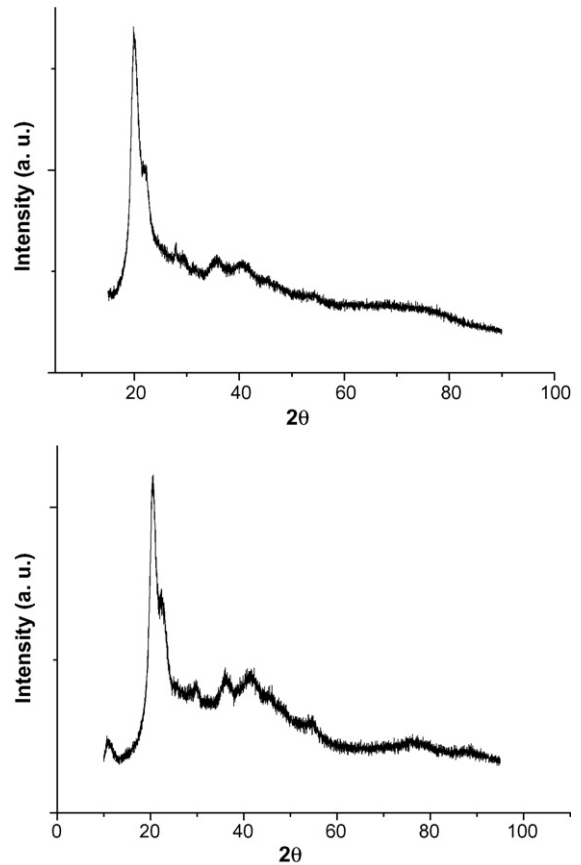


Fig. 4. DRX plots of the raw chitosan (upper panel) and cross-linked chitosan (lower panel).

### 3.2. Factorial design evaluation

A  $2^3$  full factorial design was performed to evaluate the importance of selected adsorption experimental variables. The concentration value of the metals ( $5.0 \times 10^{-3} \text{ mol L}^{-1}$ ) was chosen in order to avoid physical deposition of metals on chitosan [12]. The factor “type of metal” was evaluated due to the significant differences observed in adsorption amounts depending on the kind of metal, bonded to chitosan and chitosan derivatives via coordinative covalent bonds [7,21,23]. The amount of adsorbent (chitosan in this work) has also been observed as an important parameter to contribute with different levels of adsorbed quantities [22]. Notation that the factors used in this work have never been investigated simultaneously using factorial designs, and they were chosen for their roles, as determined previously using one-variable-at-a-time experimental procedures [3,4,7]. All factorial designs were executed in random order to correctly evaluate experimental errors [25].

The results obtained in a factorial design depend, in part, on the ranges of the factors studied. The chosen levels should be large enough to provoke response changes that are larger than experimental error. However, these differences should not be so large that quadratic or higher order effects due to the individual factors become important and invalidate the factorial model [25].

Principal and interaction effect values are easily calculated from factorial design results. Both types of effects are calculated

Table 2  
Quantitative adsorption results ( $N_f$ )<sup>a</sup> of the 2<sup>3</sup> factorial design for the interactions of metals with chitosan

Experiments	$Q$	$M$	$T$	$N_f(1)$ ( $\times 10^{-4}$ mol g <sup>-1</sup> )	$N_f(2)$ ( $\times 10^{-4}$ mol g <sup>-1</sup> )	$N_f(m)$ ( $\times 10^{-4}$ mol g <sup>-1</sup> )	$N_f(\text{pred})^b$ ( $\times 10^{-4}$ mol g <sup>-1</sup> )
1	-1	-1	-1	6.87	6.41	6.64	5.70
2	1	-1	-1	2.79	2.84	2.82	3.35
3	-1	1	-1	3.92	3.75	3.84	4.10
4	1	1	-1	1.78	1.82	1.80	1.77
5	-1	-1	1	4.90	5.27	5.09	5.69
6	1	-1	1	3.78	3.26	3.54	3.35
7	-1	1	1	4.23	3.80	4.03	4.10
8	1	1	1	2.17	2.05	2.11	1.77

<sup>a</sup>  $N_f(1)$  and  $N_f(2)$  represent duplicate values for the number of moles adsorbed, under the same experimental conditions (mol g<sup>-1</sup>), and  $N_f(m)$  values are the respective averages.

<sup>b</sup>  $N_f(\text{pred})$  represents the adsorption results predicted from Eq. (4).

using Eq. (2) [25,26]:

$$\text{effect} = \bar{R}_{+,i} - \bar{R}_{-,i} \quad (2)$$

where  $\bar{R}_{+,i}$  and  $\bar{R}_{-,i}$  are average values of  $N_f$  for the high (+) and low (-) levels of each factor. For principal or main effects, the above averages simply refer to the results at the high (+) and low (-) levels independent of the levels of the other factors. For binary interactions  $\bar{R}_+$  is the average of results for both factors at their high and low levels whereas  $\bar{R}_-$  is the average of the results for which one of the factors involved is at the high level and the other is at the low level. In general, high-order interactions are calculated using the above equation by applying signs obtained by multiplying those for the factors involved, (+) for high and (-) for low levels. If duplicate runs are performed for each individual measurement, as done in this work, standard errors ( $E$ ) in the effect values can be calculated by [25,26]:

$$E = \left\{ \frac{\sum (d_i)^2}{8N} \right\}^{1/2} \quad (3)$$

where  $d_i$  is the difference between each duplicate value and  $N$  is the number of distinct experiments performed. For triplicate determinations, the error was estimated using the well-known equation for standard deviation estimated from the  $N_f$  values.

The factorial design results are in Table 2 and the respective principal and interaction effects for the first factorial design study are presented in Table 3. On average, a decrease in the chitosan mass causes an increase in the degree of adsorption observed. This is indicated by the principal effect for chitosan mass of  $-2.33 \times 10^{-4}$  mol g<sup>-1</sup>. A similar behavior of the “mass effect” was also detected by Shen and Duvnjak [27]. When both the initial concentrations of metal ions and the volume of the solutions remain unchanged, an increase in adsorbent mass in solution was found to decrease the probability for the reaction between the every active site of adsorbent and the metal ions. Consequently, the adsorption/mass ration (mol g<sup>-1</sup>) of solute decreases [27].

The effect for type of metal,  $-1.58 \times 10^{-4}$  mol g<sup>-1</sup>, represents the higher affinity of the chitosan to form immobilized copper complexes in relation to cobalt. This behavior was also clearly demonstrated by other adsorption works [23].

Table 3  
Effect values<sup>a</sup> and their standard errors<sup>a</sup> for the interactions of metals with chitosan

Effects	Calculated effects ( $\times 10^{-4} \pm 0.23$ mol g <sup>-1</sup> )
Average	3.73
Main	
$Q$	-2.33
$M$	-1.58
$T$	-0.09
Interactions	
$Q-M$	0.35
$Q-T$	0.60
$M-T$	0.33
$Q-M-T$	-0.54

<sup>a</sup>The standard errors are the same for all effects. The 95% confidence intervals uncertainty is  $\pm 0.53$ .

All the interaction effect absolute values are much smaller than the chitosan mass and metal type main effects. At the 95% confidence level they are insignificant or only marginally significant. A cumulative normal probability plot of the standardized effects is given in Fig. 5 and shows that the values of the interaction effects and the temperature main effect fall on an approximately straight line centered on 0 and extending from

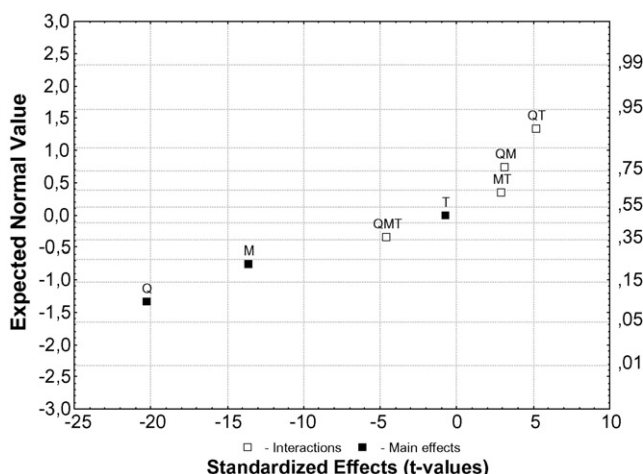


Fig. 5. Cumulative normal probability plot of the factorial design effects.



–2 to +2. This provides further evidence the corresponding values follow a normal distribution and are the consequences of experimental errors and that only the chitosan mass and metal type main effects are really significant.

### 3.2.1. Modeling of the adsorption of Cu(II) and Co(II) on the cross-linked chitosan

An approximate model for the amounts of absorbed metals (taking into account the low statistic importance of “temperature effect”, as cited earlier), calculated  $N_f$  values can be written in terms of these two significant effects ( $N_f$  units of  $10^{-4}$  mol g $^{-1}$ ) [23,26]:

$$N_f = 3.73 - 1.17x_1 - 0.79x_2 \quad (4)$$

where  $x_1$  is the quantity of chitosan and  $x_2$  is the metal type.

These models predict the same dependence of the amount of adsorbed metal on the quantity of chitosan in contact with the solution for both Cu $^{2+}$  and Co $^{2+}$ . This is a consequence of the fact that no important interaction effect was found between chitosan mass and metal type.

Analysis of variance (ANOVA) calculations (details not shown) were carried out on the above linear model and on one containing the 95% confidence level significant second- and third-order terms. In both cases significant lack of fit was observed. This indicates that there are significant curvature effects in the metal–chitosan system that can not be modeled by simple two-level factorial designs. Taking into account that it is the first attempt to study adsorption of metals on chitosan using the factorial design methodology, further statistical studies will point out a more accurate modeling to evaluate the relative importance of each experimental factor of the Cu(II) and Co(II) chitosan adsorptions. However, other adsorption parameters can also be calculated and evaluated, as described hereafter.

### 3.2.2. Thermodynamic parameters of Cu(II) and Co(II) on cross-linking chitosan

The thermodynamic parameters, namely the equilibrium constants ( $K$ ), the enthalpy of adsorption ( $\Delta_{\text{ads}}H$ ), the Gibbs free energy of adsorption ( $\Delta_{\text{ads}}G$ ) and the entropy of adsorption ( $\Delta_{\text{ads}}S$ ) were calculated as shown in Eqs. (5)–(8) [29,30], using the average adsorption quantities of the factorial design

schedule:

$$K = \frac{C_0}{C_{\text{eq}}} \quad (5)$$

$$\ln \frac{K_{35}}{K_{25}} = \Delta_{\text{ads}}H \frac{T_{35} - T_{25}}{R(T_{35}T_{25})} \quad (6)$$

$$\Delta_{\text{ads}}G = -RT \ln K \quad (7)$$

$$\Delta_{\text{ads}}G = \Delta_{\text{ads}}H - T \Delta_{\text{ads}}S \quad (8)$$

where  $C_0$  is the amount of metal (mol) adsorbed on chitosan per volume used in each factorial design experiment (0.050 L) of solution,  $C_{\text{eq}}$  the equilibrium concentration (mol L $^{-1}$ ) of metal in solution,  $T$  the solution temperature (K), which was used in relation to each factorial design and  $R$  is the universal gas constant (8.314 J K $^{-1}$  mol $^{-1}$ ).

In univariate adsorption studies, the thermodynamic aspects of adsorption are directly related to the changes of the adsorption temperature [28]. However, from the multivariate viewpoint of the results found in this work, the effect of the temperature was inexpressive in relation to the calculated error. So, the adsorption thermodynamic parameters of Cu(II) and Co(II), in this work, seem to be related to the role of the effect of principal and interactive factors of the factorial design and not to the temperature effect alone.

Table 4 shows the calculated values of the thermodynamic parameters for the Cu(II) and Co(II) adsorptions to the cross-linked chitosan. The equilibrium constants are found to be different one another, due to the differences of the  $N_f$  values found in the factorial design results. The different tendencies of the solvent detachment from the coordination sites of the M(II) species, as well as the different chemical affinities of the M(II) species to the adsorption sites are also considered important parameters to produce different  $N_f$  values [32–35].

The values of  $\Delta_{\text{ads}}H$  have been indicated exothermic and endothermic adsorption processes in relation to a specific factorial design experiment. The involved adsorption steps, at equilibrium conditions, can be stated, in a simplified manner, as following [31]:

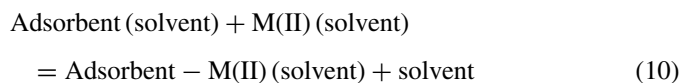


Table 4

Thermodynamic parameters of the adsorption of Cu(II) and Co(II) in relation to the 2 $^3$  factorial design<sup>a,b</sup>

Experiments	$Q$	$M$	$T$	$K$	$\Delta_{\text{ads}}H$ (kJ mol $^{-1}$ )	$\Delta_{\text{ads}}G$ (kJ mol $^{-1}$ )	$\Delta_{\text{ads}}S$ (J K $^{-1}$ mol $^{-1}$ )
1	–1	–1	–1	0.79	–17.2	0.57	–59.5
2	1	–1	–1	1.30	24.8	–0.64	85.2
3	–1	1	–1	0.34	2.58	2.64	–0.22
4	1	1	–1	0.56	10.3	1.43	29.7
5	–1	–1	1	0.51	–17.2	1.76	–59.5
6	1	–1	1	0.24	24.8	–2.34	85.2
7	–1	1	1	0.36	2.58	2.65	–0.22
8	1	1	1	0.73	10.3	0.83	29.7

<sup>a</sup> Values calculated in relation to the average equilibrium adsorption quantities ( $N_f(m)$ ).

<sup>b</sup> The standard deviations are in the range of 4–7%.

Table 5

Comparative values of  $\Delta_{\text{ads}}H$  ( $\text{kJ mol}^{-1}$ ) and maximum adsorption,  $N_f$  ( $\times 10^{-3} \text{ mol g}^{-1}$ ) for some metal–adsorbent interactions in aqueous solutions, at 25 °C

Adsorbent/adsorbate	$\Delta_{\text{int}}H$ ( $\text{kJ mol}^{-1}$ )	$N_f$	References
Raw chitosan powder/Cu(II)	−41.3	0.13	[12] <sup>a</sup>
Low porous size carbon aerogel/Cu(II)	−29.8	1.88	[36]
Piperazine-modified silica gel/Cu(II)	−67.8	0.59	[37] <sup>a</sup>
Cellulose/Cu(II)	−3.72	0.15	[38]
Diamine-modified silica gel/Cu(II)	−30.3	0.36	[39] <sup>a</sup>
<i>Zooglova ramigera</i> biomass powder/Cu(II)	−92.6	0.50	[40]
<i>Rhizopus arrhizus</i> biomass powder/Cu(II)	−67.8	0.40	[40]
Goethite/Cu(II)	−30.0	0.11	[41]
Raw chitosan powder/Cu(II)	−39.0	0.38	[42] <sup>a</sup>
Fe <sub>3</sub> O <sub>4</sub> –chitosan nanoparticles/Cu(II)	−6.2	0.10	[43]
Cellulose–chitosan thin membranes/Cu(II)	−2.1	1.92	[44] <sup>a</sup>
Vanillin–chitosan thin membranes/Cu(II)	−2.6	0.93	[45]
Rubber wood sawdust–H <sub>3</sub> PO <sub>4</sub> activated/Cu(II)	−68.2	0.10	[46]
Chitosan powder/Cr(VI)	−20.7	0.20	[47]
Chitosan cross-linked/Cu(II)	−17.2	0.66	This work
Chitosan cross-linked/Cr(VI)	+18.0	0.25	[47]
Chitosan cross-linked/Co(II)	+10.3	0.21	This work
<i>N</i> -(2-Pyridyl)acetamide-modified silica gel/Cu(II)	−127.9	0.12	[48] <sup>a,b</sup>
<i>N</i> -(2-Pyridyl)acetamide-modified silica gel/Co(II)	−20.8	0.16	[48] <sup>a,b</sup>
Zeolite MCM-22/basic dye	+5.4	0.17	[49]
Chitosan cross-linked/Co(II)	+2.6	0.38	This work
Activated carbon from co-mingled wastes/Cr(VI)	+11.1	0.49	[50]
Chitosan cross-linked/Cu(II)	+24.8	0.28	This work
<i>Pseudomonas putida</i> microorganism/Cu(II)	+23.1	1.24	[51]
Kaolinite/Cu(II)	+39.5	0.34	[52]

<sup>a</sup> Determinations performed by direct isothermal titration calorimetry.

<sup>b</sup> The solvent used was anhydrous ethanol.

For the sake of comparison, Table 5 presents comparative values of  $\Delta_{\text{ads}}H$  for some metals–adsorbent interactions. In general, it has been observed that high exothermic  $\Delta_{\text{ads}}H$  values (more than  $-29 \text{ kJ mol}^{-1}$ ) are found for M(II) adsorptions that occur, mainly, on the surfaces of low-size porous adsorbents. On the other hand, the diffusion of M(II) ions into the internal parts of the non-powdered adsorbent materials provokes endothermic and/or very small exothermic values of  $\Delta_{\text{ads}}H$ . So, the wide range of the comparative results of the  $\Delta_{\text{ads}}H$  in Table 5 (some of them obtained by direct isothermal titration calorimetry) should be seen as an evidence that the adsorption thermodynamic values are average results of both the diffusional (endothermic) and chemical bonding (exothermic) processes [29,30]. In addition, the interactive role of the experimental variables, provided in the present work by the factorial design methodology, should

also be taking into account to evaluate the changes of the  $\Delta_{\text{ads}}H$  values.

Positive (experiments 2, 4, 6 and 8 in this work) or very low negative (experiments 3 and 7 in this work)  $\Delta_{\text{ads}}S$  values, as well as the very small  $\Delta_{\text{ads}}G$  values found in this work have also been considered as the consequence of the diffusion of the M(II) species into the cross-linked chitosan [29,30,40,42,48]. In general, high negative  $\Delta_{\text{ads}}G$  values are found when adsorption occurs, mainly, at surfaces of the adsorbents [12,18,20,36,37,39,40,42,48].

#### 4. Conclusions

The results obtained in this study show that the changes proposed in the factorial design study affected the adsorption levels of Cu(II) and Co(II) by using cross-linked chitosan. The factorial studied pointed out that chitosan presents higher adsorption affinity for Cu(II) in relation to Co(II).

The results for both metals show that at the same contact time, lower adsorption capacities were reached in the factorial design experiments when higher chitosan masses are used. Furthermore, when the adsorbent concentration in solution is higher, the removal efficiency is higher, but the adsorption/mass unit ratio is lower. The “temperature effect” was inexpressive in relation to the calculated error. So, the changes of the adsorption thermodynamic parameters of Cu(II) and Co(II), in this work, seem to be related to the role of the effect of principal and interactive factors of the factorial design and not to the temperature effect alone.

Adsorption works presented in literature [44,45,47,50,51] present  $\Delta_{\text{ads}}H$  values from +11.1 to +39.5  $\text{kJ mol}^{-1}$ ,  $\Delta_{\text{ads}}G$  from  $-13.7$  to +2.75  $\text{kJ mol}^{-1}$  and  $\Delta_{\text{ads}}S$  from +0.12 to +113.4  $\text{J K}^{-1} \text{ mol}^{-1}$ . So, the thermodynamic results presented in present work, which are almost all endothermic in nature, seem to be in good agreement with the adsorption studies found in literature.

The factorial design methodology is useful to show different values of adsorption parameters, for Cu(II) and Co(II), suggest that the factorial design methodology is useful to find significant alterations in the adsorption thermodynamic parameters for interactions at the solid/solution interface.

#### Acknowledgements

The authors thank the Brazilian National Agency CNPq for fellowship to A.R.C., and The Primex Ingredients A.S. (Norway/Iceland) for both the free-gift high-quality chitosan sample and the continuous support to our research group.

#### References

- [1] United States Environmental Protection Agency (USEPA), National Primary Drinking Water Regulations, USEPA, USA, 1992.
- [2] G. Crini, Recent developments in polysaccharide-based materials used as adsorbents in wastewater treatment, Prog. Polym. Sci. 30 (2005) 38–70.
- [3] E. Guibal, Interactions of metal ions with chitosan-based sorbents: a review, Separ. Purif. Technol. 38 (2004) 43–74.

- [4] E. Guibal, Heterogeneous catalysis on chitosan-based materials: a review, *Prog. Polym. Sci.* 30 (2005) 71–109.
- [5] A.J. Varma, S.V. Deshpande, J.F. Kennedy, Metal complexation by chitosan and its derivatives: a review, *Carbohydr. Polym.* 55 (2004) 77–93.
- [6] R.A.A. Muzzarelli, *Natural Chelating Polymers: Alginic Acid, Chitin and Chitosan*, Pergamon Press, Oxford, 1973.
- [7] H.K. No, S.P. Meyers, Application of chitosan for treatment of wastewaters, *Rev. Environ. Contam. Toxicol.* 163 (2000) 1–28.
- [8] W.Q. Sun, G.F. Payne, M.S.G.L. Moas, J.H. Chu, K.K. Wallace, Tyrosinase reaction/chitosan adsorption for removing phenols from wastewater, *Biotechnol. Prog.* 8 (1992) 179–186.
- [9] J.M.C.S. Magalhães, A.A.S.C. Machado, Urea potentiometric biosensor based on urease immobilized on chitosan membranes, *Talanta* 47 (1998) 183–191.
- [10] X. Zeng, E. Ruckenstein, Cross-linked macroporous chitosan anion-exchange membranes for protein separations, *J. Membr. Sci.* 148 (1998) 195–205.
- [11] R.S. Juang, F.C. Wu, R.L. Tseng, Solute adsorption and enzyme immobilization on chitosan beads prepared from shrimp shell wastes, *Biores. Technol.* 80 (2001) 187–193.
- [12] O.A.C. Monteiro Jr., C. Airoidi, Some thermodynamic data on copper–chitin and copper–chitosan biopolymer interactions, *J. Colloid Interf. Sci.* 212 (1999) 212–219.
- [13] N. Karatepe, Adsorption of a non-ionic dispersant on lignite particle surfaces, *Energy Conver. Manage.* 44 (2003) 1275–1284.
- [14] S. Chegrouche, A. Bensmaili, Removal of Ga(III) from aqueous solution by adsorption on activated bentonite using a factorial design, *Water Res.* 36 (2002) 2898–2904.
- [15] G. Annadurai, R.S. Juang, D.J. Lee, Factorial design analysis for adsorption of dye on activated carbon beads incorporated with calcium alginate, *Adv. Environ. Res.* 6 (2002) 191–198.
- [16] G. Nicholls, B.J. Clark, J.E. Brown, Solid-phase extraction and optimized separation of doxorubicin, epirubicin and their metabolites using reversed-phase high-performance liquid chromatography, *J. Pharm. Biomed. Anal.* 10 (1992) 949–957.
- [17] D. de Brito, S.P. Campana, A kinetic study on the thermal degradation of *N,N,N*-trimethylchitosan, *Polym. Degrad. Stab.* 84 (2004) 353–361.
- [18] O.A.C. Monteiro Jr., C. Airoidi, The influence of chitosans with defined degrees of acetylation on the thermodynamic data for copper coordination, *J. Colloid Interf. Sci.* 282 (2005) 32–37.
- [19] O. Leal, C. Bolívar, C. Ovalles, J.J. Garcia, Y. Espidel, Reversible adsorption of carbon dioxide on amine surface-bonded silica gel, *Inorg. Chim. Acta* 240 (1995) 183–189.
- [20] E.F.S. Vieira, A.R. Cestari, J.A. Simoni, C. Airoidi, Thermochemical data for interaction of some primary amines with complexed mercury on mercapto-modified silica gel, *Thermochim. Acta* 399 (2003) 121–126.
- [21] E.C.N. Lopes, F.S.C. dos Anjos, E.F.S. Vieira, A.R. Cestari, An alternative Avrami equation to evaluate kinetic parameters of the interaction of Hg(II) with thin chitosan membranes, *J. Colloid Interf. Sci.* 263 (2003) 542–547.
- [22] A.R. Cestari, E.F.S. Vieira, R.E. Bruns, C. Airoidi, Some new data for metal desorption on inorganic–organic hybrid materials, *J. Colloid Interf. Sci.* 227 (2000) 66–70.
- [23] A.R. Cestari, E.F.S. Vieira, E.S. Silva, Interactions of anionic dyes with silica–aminopropyl. 1. A quantitative multivariate analysis of equilibrium adsorption and adsorption Gibbs free energies, *J. Colloid Interf. Sci.* 297 (2006) 22–30.
- [24] A.R. Cestari, E.F.S. Vieira, A.G.P. dos Santos, J.A. Mota, V.P. de Almeida, Adsorption of anionic dyes on chitosan beads. 1. The influence of the chemical structures of dyes and temperature on the adsorption kinetics, *J. Colloid Interf. Sci.* 280 (2004) 380–386.
- [25] G.P.G. Box, W.G. Hunter, J.S. Hunter, *Statistics for Experimenters: An Introduction for Design, Data Analysis and Model Building*, John Wiley & Sons, New York, 1978.
- [26] A.R. Cestari, E.F.S. Vieira, A.J.P. Nascimento, C. Airoidi, New factorial designs to evaluate chemisorption of divalent metals on aminated silicas, *J. Colloid Interf. Sci.* 241 (2001) 45–51.
- [27] J. Shen, Z. Duvnjak, Adsorption kinetics of cupric and cadmium ions on corn cob particles, *Process Biochem.* 40 (2005) 3446–3454.
- [28] Y.-S. Ho, A.E. Ofomaja, Kinetics and thermodynamics of lead ion sorption on palm kernel fibres from aqueous solution, *Process Biochem.* 40 (2005) 3455–3461.
- [29] S.S. Tahir, N. Rauf, Thermodynamic studies of Ni(II) adsorption onto bentonite from aqueous solution, *J. Chem. Thermodyn.* 35 (2003) 2003–2009.
- [30] E. Gimenez-Martin, M. Espinosa-Jiménez, Influence of tannic acid in leacril/rhodamine B system: thermodynamics aspects, *Colloids Surf. A* 270/271 (2005) 93–101.
- [31] I.S. Lima, C. Airoidi, A thermodynamic investigation on chitosan–divalent cation interactions, *Thermochim. Acta* 421 (2004) 133–139.
- [32] D. Mohan, C.U. Pittman Jr., P.H. Steele, Single, binary and multi-component adsorption of copper and cadmium from aqueous solutions on Kraft lignin—a biosorbent, *J. Colloid Interf. Sci.* 297 (2006) 489–504.
- [33] M. El-Batouti, O.M. Sadek, F.F. Assaad, Kinetics and thermodynamics studies of copper exchange on Na–montmorillonite clay mineral, *J. Colloid Interf. Sci.* 259 (2003) 223–227.
- [34] J. Burgess, *Metal Ions in Solution*, John Wiley & Sons, New York, 1978.
- [35] J. Romero-Gonzalez, J.R. Peralta-Videa, E. Rodriguez, S.L. Ramirez, J.L. Gardea-Torresdey, Determination of thermodynamic parameters of Cr(VI) adsorption from aqueous solution onto *Agave lechuguilla* biomass, *J. Chem. Thermodyn.* 37 (2005) 343–347.
- [36] A.K. Meena, G.K. Mishra, P.K. Rai, C. Rajagopal, P.N. Nagar, Removal of heavy metal ions from aqueous solutions using carbon aerogel as an adsorbent, *J. Hazard. Mater. B* 122 (2005) 161–170.
- [37] J.G.P. Espinola, L.N.H. Arakaki, S.F. Oliveira, M.G. da Fonseca, J.A.A. Campos Filho, C. Airoidi, Some thermodynamic data of the energetics of the interaction cation–piperazine immobilized on silica gel, *Colloids Surf. A* 221 (2003) 101–108.
- [38] Y.-C. Chang, D.-H. Chen, Preparation and adsorption properties of monodisperse chitosan-bound Fe<sub>3</sub>O<sub>4</sub> magnetic nanoparticles for removal of Cu(II) ions, *J. Colloid Interf. Sci.* 283 (2005) 446–451.
- [39] O. Yavuz, Y. Altunkaynak, F. Guzel, Removal of copper, nickel, cobalt and manganese from aqueous solution by kaolinite, *Water Res.* 37 (2003) 948–952;
- A.R. Cestari, E.F.S. Vieira, J.A. Simoni, C. Airoidi, Thermochemical investigation on the adsorption of some divalent cations on modified silicas obtained from sol–gel process, *Thermochim. Acta* 348 (2000) 25–31.
- [40] Y. Sag, T. Kutsal, Determination of the biosorption heats of heavy metal ions on *Zoogloea ramigera* and *Rhizopus arrhizus*, *Biochem. Eng. J.* 6 (2000) 145–151.
- [41] B. Acemioğlu, M.H. Alma, Equilibrium studies on adsorption of Cu(II) from aqueous solution onto cellulose, *J. Colloid Interf. Sci.* 243 (2001) 81–84.
- [42] I.S. Lima, C. Airoidi, Interaction of copper with chitosan and succinic anhydride derivative—a factorial design evaluation of the chemisorption process, *Thermochim. Acta* 421 (2004) 133–139.
- [43] D.P. Rodda, J.D. Wells, B.B. Johnson, Anomalous adsorption of Copper(II) on goethite, *J. Colloid Interf. Sci.* 184 (1996) 564–569.
- [44] I.S. Lima, A.M. Lazzarin, C. Airoidi, Favorable chitosan/cellulose film combinations for copper removal from aqueous solutions, *Int. J. Biol. Macromol.* 36 (2005) 79–83.
- [45] A.R. Cestari, E.F.S. Vieira, C.R.S. Matos, Thermodynamics of adsorption of Cu(II) on vanillin-modified thin chitosan membranes, *J. Chem. Thermodyn.* 38 (2006) 1092–1099.
- [46] M.H. Kalavathy, T. Karthikeyan, S. Rajgopal, L.R. Miranda, Kinetic and isotherm studies of Cu(II) adsorption onto H<sub>3</sub>PO<sub>4</sub>-activated rubber wood sawdust, *J. Colloid Interf. Sci.* 292 (2005) 354–362.
- [47] S.P. Ramnani, C.V. Chaudhari, N.D. Patil, S. Sabharwal, Synthesis and Characterization of cross-linked chitosan formed by gamma irradiation in the presence of carbontetrachloride as a sensitizer, *J. Polym. Sci. A* 42 (2004) 3897–3909.
- [48] C. Airoidi, E.F.C. Alcântara, Chemisorption of divalent cations on *N*-(2-pyridyl)acetamide immobilized on silica gel—a thermodynamic study, *J. Chem. Thermodyn.* 27 (1995) 623–632.



- [49] S. Wang, H. Li, L. Xu, Application of zeolite MCM-22 for basic dye removal from wastewater, *J. Colloid Interf. Sci.* 295 (2006) 71–78.
- [50] S.I. Lyubchik, A.I. Lyubchik, D.L. Galushka, L.P. Tikhonova, J. Vital, I.M. Fonseca, S.B. Lyubchik, Kinetics and thermodynamics of the Cr(III) adsorption on the activated carbon from co-mingled wastes, *Colloids Surf. A* 242 (2004) 151–158.
- [51] G. Uslu, M. Tanyol, Removal of Cu(II) using *Pseudomonas putida*, *J. Hazard. Mater. B* 135 (2006) 87–93.
- [52] O. Yavuz, Y. Altunkaynak, F. Guzel, Removal of copper, nickel, cobalt and manganese from aqueous solution by kaolinite, *Water Res.* 37 (2003) 948–952.